THE JOURNAL OF BIOLOGICAL CHEMISTRY VOL. 283, NO. 16, pp. 10671–10678, April 18, 2008

Cholix Toxin, a Novel ADP-ribosylating Factor from *Vibrio cholerae*[*] [S]

Received for publication, December 7, 2007, and in revised form, February 4, 2008 Published, JBC Papers in Press, February 14, 2008, DOI 10.1074/jbc.M710008200

René Jørgensen[‡1,2], Alexandra E. Purdy[§1,3], Robert J. Fieldhouse[‡], Matthew S. Kimber[‡], Douglas H. Bartlett[§4], and A. Rod Merrill[‡5]

From the [‡]Department of Molecular and Cellular Biology, University of Guelph, Guelph, Ontario N1G 2W1, Canada and the [§]Marine Biology Research Division, Center for Marine Biotechnology and Biomedicine, Scripps Institution of Oceanography, University of California, San Diego, La Jolla, California 92093-0202

The ADP-ribosyltransferases are a class of enzymes that display activity in a variety of bacterial pathogens responsible for causing diseases in plants and animals, including those affecting mankind, such as diphtheria, cholera, and whooping cough. We report the characterization of a novel toxin from *Vibrio cholerae*, which we call cholix toxin. The toxin is active against mammalian cells (IC_{50} = 4.6 ± 0.4 ng/ml) and crustaceans (*Artemia nauplii* LD_{50} = 10 ± 2 μg/ml). Here we show that this toxin is the third member of the diphthamide-specific class of ADP-ribose transferases and that it possesses specific ADP-ribose transferase activity against ribosomal eukaryotic elongation factor 2. We also describe the high resolution crystal structures of the multidomain toxin and its catalytic domain at 2.1- and 1.25-Å resolution, respectively. The new structural data show that cholix toxin possesses the necessary molecular features required for infection of eukaryotes by receptor-mediated endocytosis, translocation to the host cytoplasm, and inhibition of protein synthesis by specific modification of elongation factor 2. The crystal structures also provide important insight into the structural basis for activation of toxin ADP-ribosyltransferase activity. These results indicate that cholix toxin may be an important virulence factor of *Vibrio cholerae* that likely plays a significant role in the survival of the organism in an aquatic environment.

Many pathogenic bacteria utilize secreted protein toxins (exotoxins) as components of their virulence repertoire. These toxins induce cell death or alter cellular physiology by mechanisms such as proteolysis, pore formation, and covalent modification of host proteins. Although some toxins are responsible for the complete pathology of a disease, others manipulate the host immune response, promote escape from the intracellular environment, release nutrients, or facilitate bacterial penetration of host barriers (1, 2). Since secreted toxins have been best characterized in terms of their virulence toward mammals, survival of these pathogens in the environment may provide additional selective pressures. For example, the secreted phospholipase of *Pseudomonas aeruginosa* encoded by *plcS* (now known as *plcH*) contributes to virulence against *Candida albicans* (3), the greater wax moth, *Galleria mellonella* (4), *Arabidopsis*, and mice (5). Furthermore, secreted toxins may play roles in survival or colonization by non-pathogenic bacteria involved in symbioses (6).

Cholera toxin, an A-B_5 toxin that is expressed by some strains of *Vibrio cholerae*, causes cholera disease by specifically transferring an ADP-ribose group to an Arg residue of the GTP-binding protein G_s, thereby activating adenylate cyclase. Increased concentration of cAMP leads to secretion of Cl^-, HCO_3^-, and water from epithelial cells at the site of colonization, resulting in dehydration and electrolyte loss from the infected patient. Production of a "rice stool" by these patients, which carries *V. cholerae* at concentrations as high as 10^8/ml (7), promotes dissemination of the disease among people without access to clean drinking water. Cholera cases have been linked to physical and biological conditions present in aquatic environments (8–10), and the bacterium is now known to be a constituent of the aquatic microbial community (11). Thus far, only two serogroups (O1 and O139, of more than 200 known) are thought to have been responsible for the seven pandemics occurring since 1817 (11). In the environment, most strains of other serogroups (non-O1, non-O139), do not carry the genes encoding cholera toxin, and exhibit considerable genetic diversity. These strains are known to be capable of carrying many additional virulence factors, including hemolysin (12), repeats in the structural toxin (13), heat-stable enterotoxin (14), hemagglutinin/protease (15), a type III secretion system (16), and a novel type VI secretion system associated with virulence (17), and have caused sporadic outbreaks of gastrointestinal disease distinct from cholera (18, 19) as well as extra-intestinal infections (20). However, unsuccessful attempts to correlate

* The costs of publication of this article were defrayed in part by the payment of page charges. This article must therefore be hereby marked "*advertisement*" in accordance with 18 U.S.C. Section 1734 solely to indicate this fact.

The atomic coordinates and structure factors (codes 2Q5T and 2Q6M) have been deposited in the Protein Data Bank, Research Collaboratory for Structural Bioinformatics, Rutgers University, New Brunswick, NJ (http://www.rcsb.org/).

[S] The on-line version of this article (available at http://www.jbc.org) contains supplemental Fig. S1 and Table S1.

[1] Both authors contributed equally to this work.

[2] Supported by Canadian Institutes for Health Research (CIHR) and Carlsberg Foundation fellowships.

[3] Recipient of a pre-doctoral fellowship from Howard Hughes Medical Institute.

[4] Supported by National Institutes of Health Grant AI46600-02 and University of California Marine Council Grant CEQI0047. To whom correspondence may be addressed: Marine Biology Research Division, Center for Marine Biotechnology and Biomedicine, 8750 Biological Grade Scripps Institution of Oceanography, University of California-San Diego, La Jolla, CA 92093-0202. Tel.: 858-534-5233; Fax: 858-534-7313; E-mail: dbartlett@ucsd.edu.

[5] Supported by CIHR and Canadian Cystic Fibrosis Foundation. To whom correspondence may be addressed: Dept. of Molecular and Cellular Biology, University of Guelph, Science Complex, 50 Gordon St., Guelph, Ontario N1G 2W1, Canada. Tel.: 519-824-4120 (ext. 53805); Fax: 519-837-1802; E-mail: rmerrill@uoguelph.ca.

genotypes of non-O1, non-O139 *V. cholerae* isolates with their virulence phenotypes in rabbit and mouse models suggest the presence of additional virulence factors (12). Detailed analyses of the genomes of specific non-O1, non-O139 strains of environmental origin (21) and clinical origin (22) have revealed the presence of a gene (*chxA*) encoding a novel putative secreted exotoxin (23), with similarity to exotoxin A (ExoA)[6] of *P. aeruginosa*. ExoA is a potent ADP-ribosylating toxin that specifically modifies the post-translationally modified histidine residue, diphthamide, in the essential eukaryotic ribosomal elongation factor 2 (eEF2) (24). The ADP-ribose moiety of NAD^+ is transferred onto the diphthamide imidazole leading to inhibition of protein synthesis in susceptible eukaryotic cells (25, 26). Herein, we clearly demonstrate that the *chxA* gene encodes a second major ADP-ribosylating toxin in *V. cholerae.* This toxin is catalytically active, specific for the ribosomal eEF2 substrate, and toxic against a diverse array of eukaryotes. Cholix toxin is only the third member of the eEF2-specific ADP-ribosyltransferase toxins, in addition to ExoA and diphtheria toxin (DT). Finally, we have determined the crystal structures of the full-length cholix toxin and its catalytic C-terminal domain ($cholix_c$) to 2.1 Å and 1.25 Å, respectively. Remarkably, the latter structure is the highest resolution to date for any member of the ADPRT family and is co-crystallized in complex with a competitive inhibitor, PJ34, which binds to the NAD^+ binding pocket of the toxin. Furthermore, the full-length structure demonstrates striking similarities to ExoA, which consists of a tripartite domain structure, including domains I–III that function in receptor binding, membrane translocation, and enzyme catalysis, respectively. The new crystal structures reveal that inherent flexibility of Loop 1 (L1) (and perhaps also Loop 4, L4) in the toxin is a prerequisite for enzymatic activity and that disruption of specific H-bonds to domain II, either from reduction of disulfide bonds, from furin cleavage or both, is what activates the toxin upon entry into the eukaryotic host cell. In agreement with recent structural studies of the eEF2·ExoA·NAD^+ complex,[7] L1 of cholix toxin also has the potential to interact with both NAD^+ and the diphthamide target residue in eEF2 to form a solvent cover for the active site during the transferase reaction.

EXPERIMENTAL PROCEDURES

Cloning of chxA Gene, Expression, and Purification of Cholix and $Cholix_c$ Toxins—The 208-residue catalytic fragment of cholix toxin ($cholix_c$) gene (GB AY876053) was cloned into a pET-28a(+) vector with a N-terminal His_6 tag and a Tobacco Etch Virus protease site. *Escherichia coli* ER2566 cells were transformed with plasmid and were harvested by centrifugation, resuspended in 50 mM Tris-HCl, pH 7.6, 200 mM NaCl, 0.1% Tween, 1.25 mM phenylmethylsulfonyl fluoride and lysed in a French press. The cell lysate was centrifuged at 4 °C at 20,000 × *g* for 20 min, twice. The filtered supernatant was loaded onto a nickel-charged HiTrap™ Chelating HP column (GE Healthcare) equilibrated in 20 mM Tris-HCl, pH 7.9, and 500 mM NaCl, washed with buffer and eluted with a 0–250 mM imidazole gradient. The $cholix_c$ toxin was dialyzed in 20 mM Tris-HCl, pH 7.6, 200 mM NaCl, and 0.1 mM phenylmethylsulfonyl fluoride and was digested with tobacco etch virus (1:10 ratio) at 4 °C. The protein was then separated on a HiTrap™ Chelating HP column, and the flow-through was loaded onto a Mono Q column (Amersham Biosciences) in 20 mM Tris-HCl, pH 7.6, 10% glycerol, and 25 mM NaCl and eluted with a 25–500 mM NaCl gradient.

The gene encoding the 634-residue cholix toxin for structural studies (GB AY876053) was cloned into a pET-28a(+) vector with a N-terminal His_6 tag. The cells were expressed and purified as for the catalytic fragment. The cholix toxin for *in vivo* studies was produced from a different construct possessing a tobacco etch virus protease digestion site between the His_6 tag and the protein sequence. The His_6 tag was cleaved off the full-length cholix toxin by tobacco etch virus digestion as described for the catalytic fragment. The $cholix_c$ and cholix toxins were both concentrated to ~7 mg/ml in 100 mM NaCl, 20 mM Tris-HCl, pH 7.2, buffer.

Cytotoxicity Assays—Mouse L-M fibroblasts (ATCC CCL-1.2) were maintained at 37 °C (5% CO_2) in modified McCoy 5A media supplemented with 10% fetal calf serum, 125 units/ml penicillin, 125 μg/ml streptomycin, 25 mM HEPES, and 2 mM L-glutamine. Cells were added to 24-well cell culture dishes (1×10^5 cells/ml) and were incubated for 5 h, washed with fresh media, and incubated with 0.75 ml of media containing 1 μCi/ml of L-[4,5-^{3}H]leucine (GE Healthcare) for 18 h. Cells were washed twice with 0.5 ml phosphate-buffered saline, and 0.25 ml of 0.1 N NaOH was added. After 5 min at 37 °C, 4 wells of each treatment were pooled together and transferred to microcentrifuge tubes. Protein was precipitated with sodium deoxycholate and 7% trichloroacetic acid, and the precipitate was washed twice with 6% trichloroacetic acid, prior to dissolving in 0.2–0.4 ml of 0.1 N NaOH for 30 min at 56 °C. Protein concentrations were determined (Bio-Rad DC Protein Assay kit), and incorporation of [^{3}H]leucine was measured in a Beckman LS6000TA scintillation counter (Ultima Gold mixture, PerkinElmer Life Sciences). For Fig. 1, toxin was added at the indicated dilutions in fresh media and incubated with the cells for ~48 h.

Cytotoxicity Assays Comparing MEF-1 and PEA13 Cells—MEF-1 and PEA 13 cells were maintained in Dulbecco's modified Eagle's medium supplemented with 10% fetal calf serum and incubated at 37 °C under 10% CO_2. Then, 5×10^5 cells/ml were added to 24-well dishes in a 1-ml volume, and experiments were performed as above, except that cells were incubated with toxin for 16 h, then with [^{3}H]leucine for 3 h. Samples were processed as above, except that ScintiSafe-30% (Fisher) scintillation mixture was utilized.

Artemia Toxicity Assays—Artemia cysts were added to filtered seawater and aerated at room temperature for ~24 h. Within several hours of hatching, *A. nauplii* were placed in 24-well dishes containing 400 μl of sterile sea water, with a total

[6] The abbreviations used are: ExoA, *P. aeruginosa* exotoxin A; $ExoA_c$, *P. aeruginosa* exotoxin A catalytic fragment; $cholix_c$, *V. cholerae* exotoxin catalytic fragment; DTA, diphtheria toxin catalytic fragment; DT, diphtheria toxin; eEF2, eukaryotic ribosomal elongation factor 2; ADPRT, ADP-ribosyltransferase; LRP, low density lipoprotein receptor-related protein; r.m.s.d., root mean square deviation.

[7] R. Jorgensen, Y. Wang, D. Visschedyk, and A. R. Merrill, submitted for publication.

of 30–70 *nauplii* per well, and incubated at 28 °C for 42–45 h. *Artemia* mortality was assessed using a dissecting microscope.

Detection of Biotinylated ADP-ribose-eEF2—100 μM Bio-NAD (Trevigen) was incubated with 5 μM toxin in the presence of 7 μl of CHO cell lysate in 60 mM Tris-HCl, pH 7.6, buffer for 60 min at 25 °C. The proteins were separated on by SDS-PAGE (27) and were transferred to nitrocellulose at 125 mA for 80 min. The membrane was blocked (2% bovine serum albumin in phosphate-buffered saline) for 1 h and then was incubated in 0.5% bovine serum albumin in phosphate-buffered saline with 1:5000 dilution of streptavidin-alkaline phosphate conjugate (Promega) and mixed overnight on a Nutator at 4 °C. The blot was then washed with 0.5 mM $MgCl_2$, 40 mM $NaHCO_3$, pH 9.6, buffer and developed in 10 ml of 5-bromo-4-chloro-3-indolyl phosphate/nitro blue tetrazolium alkaline phosphate substrate for 3 min.

Crystallography—The cholix$_c$ toxin was co-crystallized with 5 mM PJ34 (Sigma-Aldrich) by vapor diffusion against reservoirs containing 15% polyethylene glycol-8000 and 20 mM KH_2PO_4 at 19 °C. Before flash freezing in liquid N_2, the crystals were transferred to paratone-N (Hampton research) for cryoprotection. A native 1.25-Å dataset was collected at Advanced Photon Source beamline 19-ID, and a 1.65-Å dataset on a crystal soaked for 1 h in 5 mM $HgCl_2$ was collected at beamline 17-ID. The cholix$_c$ toxin structure was solved using single-wavelength anomalous dispersion phases. The anomalous scattering substructure search, density modification, and initial chain tracing were all performed in Phenix (28), and a single major and two minor sites were found. The resulting partial model was used for molecular replacement against the high resolution native dataset using the CCP4 program MolRep (29), and the structure was then traced using warpNtrace (30) and was iteratively rebuilt in Coot (31) and anisotropically refined in Refmac5 (32) at 1.25-Å resolution.

Cholix toxin was crystallized by vapor diffusion against reservoirs containing 23% polyethylene glycol-10,000, 7.5% ethylene glycol, and 0.1 M HEPES, pH 7.5, at 19 °C. Before flash freezing in liquid N_2 the crystals were transferred to paratone-N (Hampton research) for cryoprotection. A native 2.1-Å dataset was collected at our in-house Enraf-Nonius FR571 diffractometer equipped with a rotating copper anode and a Proteum Pt135 CCD detector (Bruker). The structure of cholix toxin was solved by molecular replacement with CNS 1.1 (33) and Phaser (34) using the refined structure of cholix$_c$ toxin together with the receptor binding and translocation domains from the structure of ExoA from *P. aeruginosa* (PDB entry 1IKQ) as search models. The solution from molecular replacement was used as input to warpNtrace, which could trace ~80% of the structure. The model was rebuilt in Coot and refined in Refmac5 using TLS at 2.1-Å resolution.

RESULTS AND DISCUSSION

chxA Encodes a Putative ADPRT—Previously, we identified several DNA fragments from *V. cholerae* strains SIO and TP that have strong similarity to genes encoding virulence factors in known bacterial pathogens, including a putative ADPRT with resemblance to the *toxA* gene from *P. aeruginosa* (21). This gene, called *chxA*, encodes a 666-residue protein with a 32-residue leader sequence, called cholix toxin (70.7-kDa, 634-residue mature protein), and is similar to known diphthamide-specific ADPRTs (23). The cholix toxin primary structure shows 32% sequence identity with *Pseudomonas* ExoA, has a furin protease site for cellular activation (35), contains a C-terminal KDEL sequence that likely routes the toxin to the endoplasmic reticulum of the host cell (36), and possesses three classical signature regions (23, 37) peculiar to the catalytic domain of the diphthamide-specific toxins (23). Thus, all of these features within the primary sequence of the cholix toxin provided a powerful indication that this protein is a new member of the eEF2-specific ADPRT group (DT group) (23, 37).

Cholix Toxin Is a Bacterial ADPRT Enzyme—The ADPRT reaction in the DT group involves a nucleophilic substitution where the diphthamide imidazole in eEF2 is the nucleophile that replaces the nicotinamide base (leaving group) of the

TABLE 1

Comparison of the ADPRT kinetic parameters for ExoA$_c$ and cholix$_c$ toxins

The kinetic parameters were determined as described under "Experimental Procedures." The values represent the mean ± S.D. from three independent experiments.

Parameter	ExoA$_c$	Cholix$_c$ toxin
$K_{m(NAD)}$ (μM)	121 ± 21	45 ± 3
V_{max} (M s^{-1})	1.3×10^{-7}	1.03×10^{-7}
k_{cat} (s^{-1})	13 ± 2	10 ± 3
k_{cat} (s^{-1}) catalytic Glu → Ala[a]	0.008 ± 0.0001	0.004 ± 0.003
k_{cat}/K_m (M^{-1} s^{-1})	1.1×10^5	2.3×10^5

[a] The catalytic Glu to Ala mutations involved Glu-553 (ExoA$_c$) and Glu-581 (cholix$_c$ toxin).

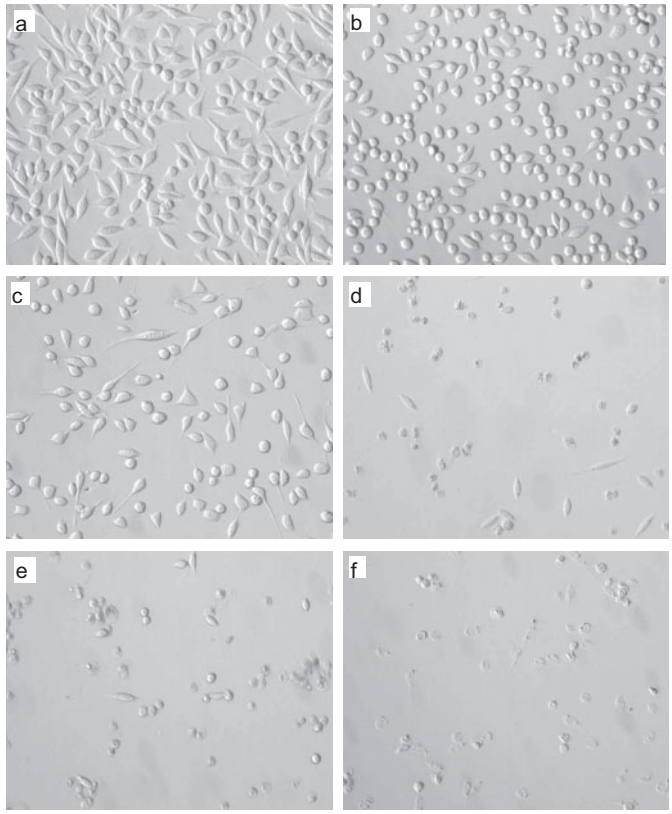

FIGURE 1. **Cholix toxin is cytotoxic toward mouse fibroblasts.** Cytotoxicity after ~48 h toxin exposure. *a*, cells display several morphotypes with no toxin. *b*, with 50 ng/ml E581A toxin cells still reach normal density. *c*, with 1 ng/ml wild-type toxin, cells are normal. *d*, 10 ng/ml; *e*, 25 ng/ml; or *f*, 50 ng/ml of wild-type toxin clearly results in cytotoxic effects.

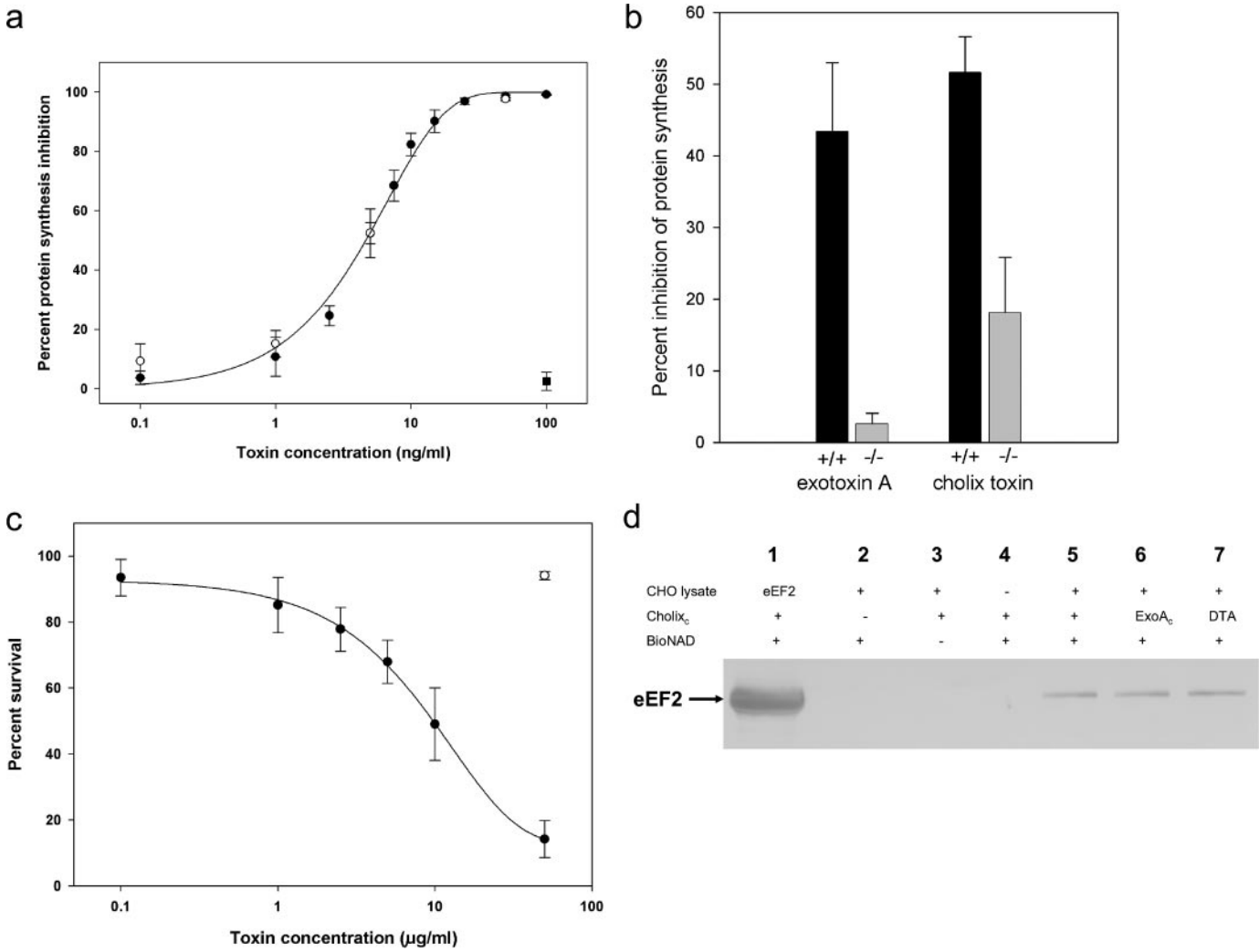

FIGURE 2. **Biological activity of cholix toxin.** *a*, protein synthesis inhibition in mouse fibroblasts. Cholix toxin (*closed circles*) inhibits protein synthesis similarly to ExoA (*open circles*) but E581A mutant (*closed squares*) does not. *b*, protein synthesis inhibition by ExoA and cholix toxin in mouse embryonic fibroblast1 (LRP1$^{+/+}$) and PEA13 (LRP1$^{-/-}$) cells at 100 ng/ml. *c*, survival (%) of *A. nauplii* exposed to cholix toxin. Cholix toxin (*closed circles*) displays a dose-dependent effect on *A. nauplii* after 42–45 h. Cholix toxin E581A (*open circle*) displays no toxic effect. *d*, Western blot showing biotin-ADP-ribose labeling of eEF2 in CHO lysate. *Lane 1*, 0.25 μg of eEF2 incubated with cholix toxin; *lanes 2–4*, various controls; *lanes 5–7*, labeling of CHO lysate by cholix$_c$ toxin, ExoA$_c$, and diphtheria toxin catalytic fragment (*DTA*), respectively.

NAD$^+$ substrate (23). The cellular effect of the covalent modification (ribosylation) of eEF2 is inhibition of protein synthesis leading to host cell death (38). To explore whether cholix toxin possessed ADPRT activity, we cloned both the full-length and truncated *chxA* gene into the T7-based *E. coli* pET28b vector for expression and purification of both the whole toxin and its C-terminal catalytic domain. The proteins were purified by immobilized metal ion chromatography and were tested for both NAD-glycohydrolase and ADPRT activities using a fluorescence-based assay with purified yeast eEF2 as substrate previously developed in our laboratory (39). The full-length recombinant toxin (634 residues, 70.7 kDa) showed only weak catalytic activity suggesting that this protein requires activation, a prerequisite for this family of enzymes/toxins (40–42). In contrast, the catalytic fragment (208 residues, 23 kDa) showed strong glycohydrolase (K_m, 67 ± 4 μM; k_{cat}, 1.92 ± 0.12 h^{-1}) and ADPRT activities (Table 1). Cholix toxin is a slightly better enzyme than ExoA with a lower K_m (3-fold), similar k_{cat}, and specificity constant (2-fold higher) for the NAD$^+$ substrate (23). Furthermore, replacing the hallmark catalytic Glu-581 residue (corresponding to Glu-553 in ExoA and Glu-148 in DT) within the enzyme domain of cholix toxin with an Ala showed the expected result on the activity of the enzyme (~2600-fold reduction in k_{cat}, Table 1). Thus, cholix toxin recognizes eEF2 as the target protein substrate and possesses both glycohydrolase and ADPRT enzyme activities, which qualifies it as the third *bone fide* member of the DT group of bacterial ADPRT enzymes along with ExoA and DT (23).

Cholix Toxin Is Active against Eukaryotic Cells—To assess whether cholix toxin possessed biological activity against eukaryotes, we dosed mouse fibroblast cells with both wild-type toxin and a catalytically inactive mutant toxin, E581A, and compared the effects on cell viability (Fig. 1). The E581A mutant toxin had little or no effect on cell viability even at high doses (50 ng/ml) (Fig. 1*b*), whereas the wild-type toxin showed considerable clearing of cell density (killing) at 1 ng/ml (Fig. 1*c*) with little or no surviving fibroblast cells at 50 ng/ml (Fig. 1*f*).

Using the cytotoxicity assay described under "Experimental Procedures," we quantified the sensitivity of mouse fibroblast 1.2 L-M cells to cholix toxin, and the results are shown in Fig. 2*a*. The

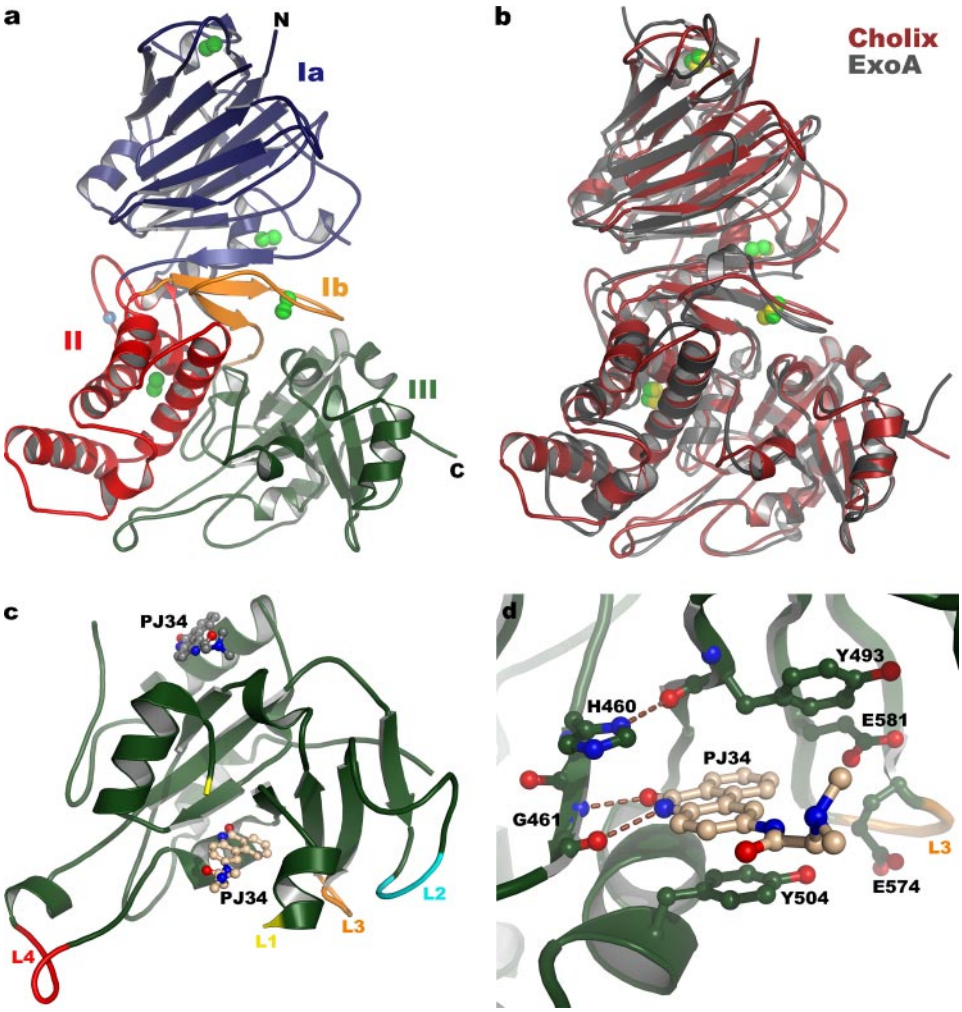

FIGURE 3. **The structure of cholix toxin.** *a*, ribbon drawing of the cholix toxin structure (PDB entry 2Q5T): domain Ia, *blue* (1–264); domain II (265–386), *red*; domain Ib (387–423), *orange*; and domain III (424–634), *green*. Disulfides and furin cut sites are shown as *light green* and *blue spheres*, respectively. *b*, superposition of ExoA onto the cholix toxin structure. Disulfides are indicated by *light green* and *yellow spheres* for cholix toxin and ExoA, respectively. *c*, ribbon drawing of the catalytic domain structure (PDB entry 2Q6M). The two PJ34 inhibitors are shown in *black* and *grey ball-and-stick* representation, and the catalytic loops (*L1–L4*) are shown in *yellow*, *cyan*, *orange*, and *red*, respectively. *d*, binding of PJ34 to the NAD^+ binding pocket. The phenyl moiety of Tyr-504 forms stacking interactions with PJ34 (4 Å), and Tyr-493 is also adjacent to the hetero-ring system.

IC_{50} is 4.6 ± 0.4 ng/ml, and this is comparable to the cytotoxicity of ExoA against this mouse fibroblast cell line (43). Furthermore, the inactive E581A mutant toxin showed little or no activity against the mouse fibroblast cells (Fig. 2*a*). The protein inhibition by ExoA and cholix toxin was also tested on mouse cells lines with and without the low density lipoprotein receptor-related protein (LRP) receptor. Fig. 2*b* shows that cholix toxin recognizes the ubiquitous LRP receptor (44), which is also the specific receptor that ExoA exploits to enter the target eukaryotic cell (45). This suggests that the cellular intoxication mechanism for cholix toxin is very similar to ExoA but differs from that of DT (46). However, because the LRP-deficient strain also showed some sensitivity to cholix toxin, it is possible that there may be other avenues, besides the LRP receptor, by which cholix toxin can access the host cell cytoplasm.

V. cholerae is an aquatic organism that is often found attached to the exoskeletons of zooplankton (47), and this behavior may provide nutrients and protection against environmental challenges (48). Therefore, we tested the ability of purified cholix toxin to act on *A. nauplii* (brine shrimp), and the results are shown in Fig. 2*c*. Remarkably, cholix toxin was toxic to *A. nauplii*, because doses near 50 μg/ml killed all of the crustaceans, yet the E581A cholix toxin mutant had no effect on their viability.

We next examined whether cholix toxin was able to specifically and covalently modify the ribosomal eEF2 protein in a mammalian cell extract. Crude extract from CHO cells was incubated with toxin in the presence of biotin-NAD^+, and the reactions were separated by SDS-PAGE, and blotted to nitrocellulose membrane and ADP-ribose-labeled bands were visualized using a streptavidin-alkaline phosphatase probe (Fig. 2*d*). The eEF2 standard protein (*lane 1*, 0.25 μg of eEF2) was labeled with biotin-ADP-ribose. Additionally, a protein corresponding to the molecular weight of mammalian eEF2 in the CHO lysate was also clearly labeled with biotin-ADP-ribose, and the labeling was dependent upon the presence of cholix toxin (*lanes 2–5*). Furthermore, both the catalytic fragment of ExoA ($ExoA_c$, residues 399–605) and DTA labeled the eEF2 protein in the CHO cell lysate (*lanes 6* and *7*). A comparable experiment involving the use of ^{32}P-labeled NAD^+ and cholix toxin gave similar results (data not shown). Thus, cholix toxin recognizes and labels only one protein in crude mammalian cell lysate that corresponds to ribosomal eEF2.

Structure of Cholix Toxin—The model of the 2.1-Å crystal structure for cholix toxin (no ligand or bound substrate) is shown in Fig. 3*a*, and it reveals that cholix toxin consists of three structural domains similar to the structure of *P. aeruginosa* ExoA. Cholix toxin has a receptor-binding domain (domain Ia, 1–264, domain Ib, 387–423 (unknown function)) that together form a 13-stranded anti-parallel β-jellyroll, a translocation domain (domain II, 265–386) consisting of a bundle of six α-helices, and a catalytic domain (domain III, 424–634) with an α/β-fold topology. As seen in ExoA, the furin cleavage site protrudes from the surface of domain II in a well ordered loop and, therefore, is readily accessible for nicking by a sequence-specific endoprotease (49). Superposition of cholix toxin onto the ExoA structure (PDB entry 1IKQ) showed an overall r.m.s.d. of 2.04 Å for the C_α atoms and 1.70, 1.58, and 1.26 Å r.m.s.d. for domains I, II, and III, respectively (Fig. 3*b*). Importantly, the positions of critical

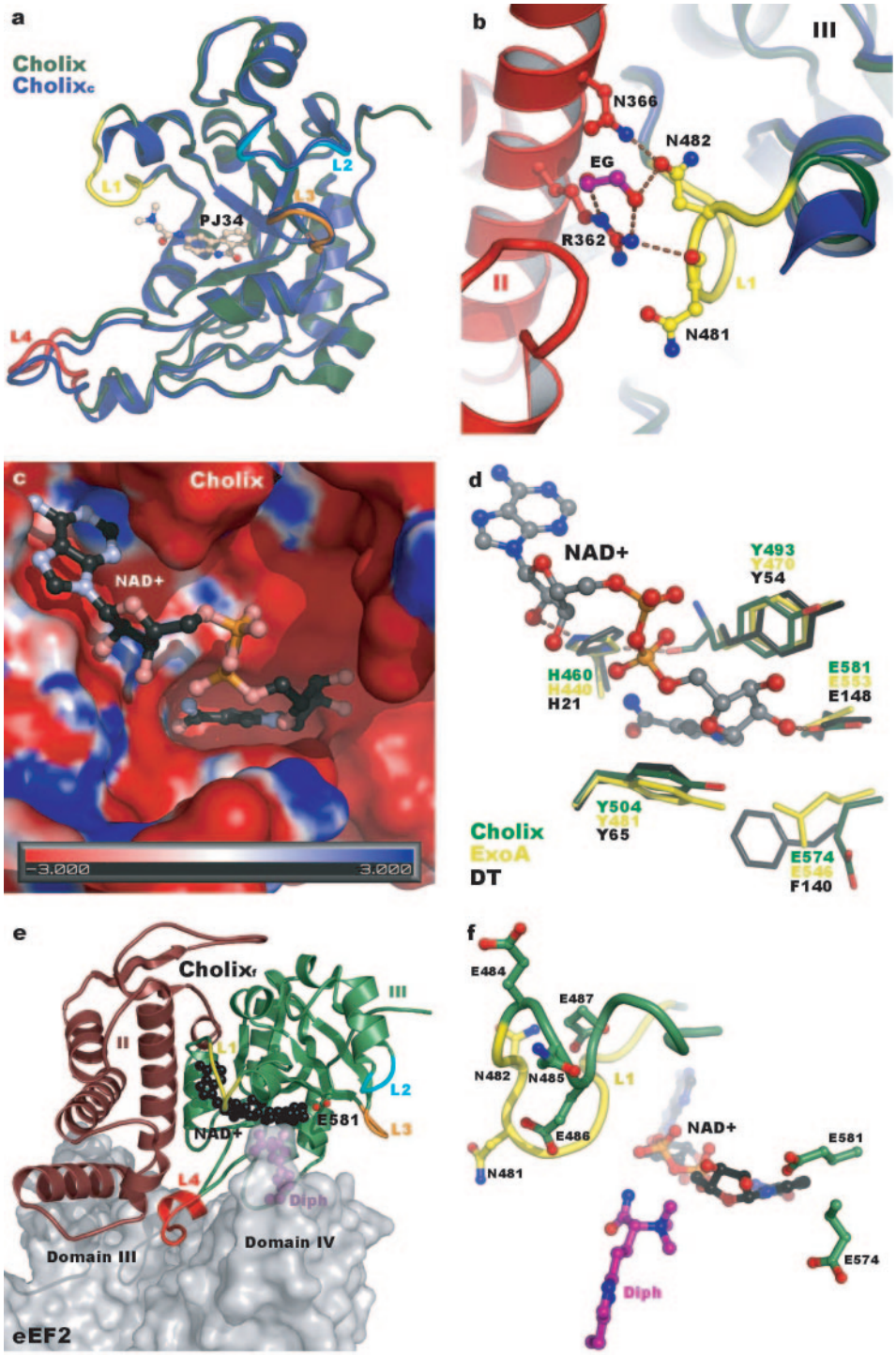

FIGURE 4. **The structure of cholix toxin.** *a*, superposition of the catalytic fragment from cholix toxin with the cholix$_c$ toxin structure (*blue*). Catalytic loops (*L1–L4* in cholix toxin) are *colored* as in Fig. 3*c* and PJ34 (*black*) in the active site is shown in *ball-and-stick* representation. *b*, L1 interactions in the cholix toxin. Asn-481 and Asn-481 (*yellow*) in L1 form H-bonds to Arg-362 and Asn-366 in α-helix E of domain II (*red*). Ethylene glycol (*purple*) mediates contact between L1 and domain II. *c*, binding of NAD^+ (*black*) to cholix$_c$ toxin from superposition of cholix$_c$ toxin onto the eEF2-ExoA-NAD^+ complex.[7] The electrostatic surface potential of the cholix toxin binding site was calculated using the APBS PyMOL plugin. *d*, superposition of catalytic fragments of DT and ExoA from eEF2-ExoA-NAD^+ onto cholix$_c$ toxin. Cholix$_c$ toxin, ExoA, and DT residues are shown as *green*, *yellow*, and *black sticks*, respectively, and NAD^+ in *grey ball-and-stick* representation. *e*, superposition of the furin-cleaved C-terminal fragment of full-length cholix toxin onto ExoA of the eEF2-ExoA-NAD^+ complex structure. Catalytic fragment (*green*) and domains Ib and II (*brown*) are shown as *ribbons*. L1–L4 are *colored* as before, and NAD^+ is in *black spheres*. eEF2 is depicted as a *white transparent surface* with the diphthamide shown in *purple spheres*. *f*, residues in L1 of cholix toxin with the potential to interact with the diphthamide and NAD^+. Same superposition and coloring as in *e*.

disulfides within cholix toxin align with those in ExoA (Fig. 3*b*), and it is clear from the cholix toxin structure that it possesses all the necessary features for a diphthamide-specific ADPRT and joins only ExoA and DT as members of this subfamily (23).

We also determined the 1.25-Å crystal structure of the catalytic fragment of cholix toxin (cholix$_c$) with PJ34 bound (Fig. 3*c*). PJ34 is a competitive inhibitor of the NAD^+ substrate for ExoA, and previously we determined its co-crystal structure with ExoA$_c$ (50). PJ34 functions both as a ligand ($K_D = 0.51\ \mu M$) and a crystallization enhancer for the cholix$_c$ toxin, and two molecules of the inhibitor can been seen in the crystal complex. Whereas one PJ34 molecule is found in the NAD^+ binding pocket as previously seen for ExoA ($K_D = 0.82\ \mu M$) (50), a second PJ34 molecule packs between two molecules of cholix$_c$ toxin in the crystal. The four catalytic loops surrounding the NAD^+ binding site (L1, 477–483; L2, 547–553; L3, 574–579; and L4, 511–518) corresponding to those in ExoA$_c$ (51) are shown in *yellow*, *cyan*, *orange*, and *red*, respectively (Fig. 3*c*). Fig. 3*d* shows the specific binding of PJ34 within the active site of cholix$_c$ toxin. The inhibitor is stabilized in the NAD^+ binding pocket through hydrophobic interactions and H-bonds. PJ34 forms two H-bonds to the backbone of Gly-461, and the phenyl moiety of Tyr-504 forms stacking interactions with the phenanthridinone ring system of PJ34. An additional H-bond is formed between His-460 and the main chain oxygen of Tyr-493 thus stabilizing these catalytic residues within the active site (Fig. 3*d*), which is also observed in the β TAD and NAD^+ complexes with toxin. The second PJ34 binds in a predominantly hydrophobic pocket formed by residues Thr-445, Leu-449, Tyr-454, Val-593, and Ile-595 in cholix$_c$ toxin molecule 1 and is held in place by Asn-550 in cholix$_c$ toxin molecule 2. Initial attempts to crystallize cholix$_c$ toxin without PJ34 failed,

suggesting that the PJ34 has an important function in stabilizing the crystal packing.

Structural Basis for Cholix Toxin Activation—It is well established that both ExoA and DT are activated within infected host cells by furin cleavage at an Arg-rich loop region along with reduction of critical disulfide bridges (52, 53) and that full-length toxin can be activated *in vitro* by urea and dithiothreitol (42, 54). Furthermore, PE40, a derivative of ExoA that is 20 residues longer than the furin-cleaved toxin, possesses two intact disulfide bonds and is enzymatically active (55). Fig. 4*a* shows the superposition of cholix$_c$ toxin with the catalytic domain of full-length toxin. The r.m.s.d. is 0.67 Å, and the only regions where the two catalytic domains do not overlap almost perfectly are at L3 (*orange*) and L4 (*red*). L4 in cholix toxin is positioned closer to domain II, where Thr-511 in L4 forms an H-bond to Asn-347 in α-helix D of domain II, and two water molecules mediate contact between Thr-518 and Glu-521 and between Asn-347 and Gly-352. L3 (*orange*) has moved slightly closer to the NAD^+ binding site in the full-length structure indicating some degree of flexibility of this loop. More importantly, the L1 residues (478–482) are not visible in the enzymatically active cholix$_c$ toxin structure, which most likely can be attributed to the highly flexible properties of this loop (Fig. 4*a*). In the full-length structure, Asn-481 and Asn-482 in L1 form H-bonds to Arg-362 and Asn-366 in α-helix E of domain II (*red*), and ethylene glycol (crystallization additive) mediates contact between L1 and domain II (Fig. 4*b*). This supports the idea that the flexibility of L1 (and perhaps also L4) is a prerequisite for enzymatic activity and that disruption of the H-bonds to domain II, either from reduction of disulfide bonds, from furin cleavage or both, is important for enzymatic activation of the toxin. A similar activation mechanism has previously been suggested for ExoA (60, 61). Although cholix$_c$ toxin was co-crystallized with the PJ34 inhibitor, NAD^+ is easily accommodated both electrostatically and stereochemically, within the NAD^+ binding site of cholix$_c$ toxin as expected for an ADPRT enzyme (Fig. 4*c*). Further evidence of the structural relationship of cholix toxin with ExoA and DT can be seen from the superposition of the catalytic domains of these three toxins (Fig. 4*d*) where the catalytic residues representing the ADPRT catalytic cluster (His-460, Tyr-493, Tyr-504, Glu-574, and Glu-581; cholix toxin residue numbering) surrounding the NAD^+ ligand have overlapping positions. Residue Glu-574 in cholix toxin has adopted a rotamer conformation, which is in agreement with the conformation of the catalytically important Glu-546 in ExoA structures without its natural NAD^+ substrate in the binding site. This indicates a similar catalytic function of Glu-574, however, the similarly positioned residue in DT (Phe-140) is not conserved and therefore likely makes use of a somewhat different reaction mechanism.

Superposition of cholix toxin, cleaved at its furin cut site, onto the eEF2·ExoA$_c$·NAD^+ complex structure reveals that L4 of cholix toxin fits snugly within the cleft between domain III and IV of eEF2 without any significant stereochemical difficulties and that L1 is positioned in an ideal location to form H-bonds with both the diphthamide and NAD^+ (Fig. 4*e*). This suggests that the molecular basis of toxin activation involves specific structural changes within the catalytic domain that involve these loop regions. In particular, L1 likely has an active role in the stabilization of the transition state possibly by moving the diphthamide into position for the nucleophilic attack of the C1 of NAD^+ and/or by functioning as a solvent cover during the enzymatic reaction. This would be in agreement with the recent structures of the eEF2·ExoA$_c$·NAD^+ mutant complexes,[7] where a Gln in L1 interacts with NAD^+ and an Asp interacts with the diphthamide in a conformation that also serves as a solvent cover. L1 in cholix toxin likewise contains residues (three Asn and three Glu) with the potential to interact with NAD^+ and the diphthamide upon activation of the toxin and NAD^+ binding (Fig. 4*f*).

In summary, DT, produced by *Corynebacterium diphtheriae*, was one of the first bacterial toxins to be investigated (46). This protein was the first member of the ADPRT family to be identified and is one of the best studied and well understood bacterial toxins (46). The closest known DT relative is ExoA, produced by *P. aeruginosa*. ExoA was discovered in the 1960s and is now believed to be the most potent toxin produced by *P. aeruginosa* (56, 57). Incredibly, DT and ExoA are only distantly related despite sharing a common ADPRT activity, target substrate protein (eEF2), and similar three-dimensional folds. Sequence similarity between the two toxins is low and is restricted to the catalytic domain. Also, the order of the domains is opposite, and the receptor-binding and translocation mechanisms are different (46).

Until recently, no other members of the DT group in the ADPRT family had been identified (21). However, as bacterial genomes are being revealed, some potential diphthamide-specific toxins have recently been identified based on a search strategy that includes a limited consensus sequence pattern combined with secondary structure prediction (23). Here we show that cholix toxin is catalytically active and specific for the eEF2 diphthamide. Remarkably, cholix toxin represents only the third member of the DT group, and it shares much greater sequence homology with ExoA than DT. Since its original discovery in environmental isolates, *chxA* has been uncovered in other *V. cholerae* strains following genome sequencing. These include clinical isolates from the U.S. and Bangladesh (22), Japan (16), and Peru as well as an environmental isolate from Bangladesh.[8] Our own analyses of strains collected in different continents confirm that the *chxA* gene is widely distributed.[9] The use of ADPRTs by *V. cholerae* is thus more extensive than previously appreciated. The specific biological target of the toxin and the nature of the symbiotic interaction associated with its activity in *V. cholerae* have yet to be determined. It could be significant that the environmental strain from which *chxA* was first discovered is capable of causing a fatal hemorrhagic pneumonia in adult mice (58). Outside of a human host, *V. cholerae* can be consumed by grazers and interacts with both phytoplankton and zooplankton. Given that some toxins can

[8] Accession numbers: NZ_AAKI00000000 (V51) (www.nmpdr.org/(NRT-36S)), NZ_AAUR00000000 (1587), NZ_AAWG00000000 (623-39), and NZ_AAWF00000000 (MZO-2).

[9] Cholix toxin is present in *V. cholerae* strains from Mexico, Bangladesh, and Peru (A. E. Purdy, D. Balch, M. L. Lizarraga-Partida, J. Martinez-Urtaza, M. S. Islam, A. Huq, R. R. Colwell, and D. H. Bartlett, unpublished data and Ref. 48).

act against multiple hosts (59), one or more of these organisms could contain the object of cholix toxin affinity and catalysis.

Acknowledgments—We thank Dawn White and Gerry Prentice for excellent technical support during this research and to Sara Kelly for help with cell culture techniques. We are grateful for help provided by the beamline staff at 17-ID and 19-ID at the Argonne Photon Source, Chicago.

REFERENCES

1. Alouf, J. E., and Freer, J. H. (1999) *The Comprehensive Sourcebook of Bacterial Protein Toxins*, 2nd Ed., Academic Press, San Diego, San Diego
2. Burns, D. L., Barbieri, J. T., Iglewski, B. H., and Rappuoli, R. (2003) *Bacterial Protein Toxins*, ASM Press, Washington, DC
3. Hogan, D. A., and Kolter, R. (2002) *Science* **296,** 2229–2232
4. Jander, G., Rahme, L. G., and Ausubel, F. M. (2000) *J. Bacteriol.* **182,** 3843–3845
5. Rahme, L. G., Stevens, E. J., Wolfort, S. F., Shao, J., Tompkins, R. G., and Ausubel, F. M. (1995) *Science* **268,** 1899–1902
6. Ruby, E. G., Urbanowski, M., Campbell, J., Dunn, A., Faini, M., Gunsalus, R., Lostroh, P., Lupp, C., McCann, J., Millikan, D., Schaefer, A., Stabb, E., Stevens, A., Visick, K., Whistler, C., and Greenberg, E. P. (2005) *Proc. Natl. Acad. Sci. U. S. A.* **102,** 3004–3009
7. Kaper, J. B., Morris, J. G., Jr., and Levine, M. M. (1995) *Clin. Microbiol. Rev.* **8,** 48–86
8. Alam, M., Hasan, N. A., Sadique, A., Bhuiyan, N. A., Ahmed, K. U., Nusrin, S., Nair, G. B., Siddique, A. K., Sack, R. B., Sack, D. A., Huq, A., and Colwell, R. R. (2006) *Appl. Environ. Microbiol.* **72,** 4096–4104
9. Huq, A., Sack, R. B., Nizam, A., Longini, I. M., Nair, G. B., Ali, A., Morris, J. G., Jr., Khan, M. N., Siddique, A. K., Yunus, M., Albert, M. J., Sack, D. A., and Colwell, R. R. (2005) *Appl. Environ. Microbiol.* **71,** 4645–4654
10. Lobitz, B., Beck, L., Huq, A., Wood, B., Fuchs, G., Faruque, A. S., and Colwell, R. (2000) *Proc. Natl. Acad. Sci. U. S. A.* **97,** 1438–1443
11. Colwell, R. R. (1996) *Science* **274,** 2025–2031
12. Faruque, S. M., Chowdhury, N., Kamruzzaman, M., Dziejman, M., Rahman, M. H., Sack, D. A., Nair, G. B., and Mekalanos, J. J. (2004) *Proc. Natl. Acad. Sci. U. S. A.* **101,** 2123–2128
13. Chow, K. H., Ng, T. K., Yuen, K. Y., and Yam, W. C. (2001) *J. Clin. Microbiol.* **39,** 2594–2597
14. Sarkar, B., Bhattacharya, T., Ramamurthy, T., Shimada, T., Takeda, Y., and Balakrish, N. G. (2002) *Epidemiol. Infect.* **129,** 245–251
15. Halpern, M., Gancz, H., Broza, M., and Kashi, Y. (2003) *Appl. Environ. Microbiol.* **69,** 4200–4204
16. Dziejman, M., Serruto, D., Tam, V. C., Sturtevant, D., Diraphat, P., Faruque, S. M., Rahman, M. H., Heidelberg, J. F., Decker, J., Li, L., Montgomery, K. T., Grills, G., Kucherlapati, R., and Mekalanos, J. J. (2005) *Proc. Natl. Acad. Sci. U. S. A.* **102,** 3465–3470
17. Pukatzki, S., Ma, A. T., Sturtevant, D., Krastins, B., Sarracino, D., Nelson, W. C., Heidelberg, J. F., and Mekalanos, J. J. (2006) *Proc. Natl. Acad. Sci. U. S. A.* **103,** 1528–1533
18. Dalsgaard, A., Albert, M. J., Taylor, D. N., Shimada, T., Meza, R., Serichantalergs, O., and Echeverria, P. (1995) *J. Clin. Microbiol.* **33,** 2715–2722
19. Sharma, C., Thungapathra, M., Ghosh, A., Mukhopadhyay, A. K., Basu, A., Mitra, R., Basu, I., Bhattacharya, S. K., Shimada, T., Ramamurthy, T., Takeda, T., Yamasaki, S., Takeda, Y., and Nair, G. B. (1998) *J. Clin. Microbiol.* **36,** 756–763
20. Dalsgaard, A., Forslund, A., Hesselbjerg, A., and Bruun, B. (2000) *Clin. Microbiol. Infect.* **6,** 625–627
21. Purdy, A., Rohwer, F., Edwards, R., Azam, F., and Bartlett, D. H. (2005) *J. Bacteriol.* **187,** 2992–3001
22. Chen, Y., Johnson, J. A., Pusch, G. D., Morris, J. G., Jr., and Stine, O. C. (2007) *Infect. Immun.* **75,** 2645–2647
23. Yates, S. P., Jorgensen, R., Andersen, G. R., and Merrill, A. R. (2006) *Trends Biochem. Sci.* **31,** 123–133
24. Jorgensen, R., Merrill, A. R., and Andersen, G. R. (2006) *Biochem. Soc. Trans.* **34,** 1–6
25. Wilson, B. A., and Collier, R. J. (1992) *Curr. Top. Microbiol. Immunol.* **175,** 27–41
26. Jorgensen, R., Yates, S. P., Teal, D. J., Nilsson, J., Prentice, G. A., Merrill, A. R., and Andersen, G. R. (2004) *J. Biol. Chem.* **279,** 45919–45925
27. Laemmli, U. K. (1970) *Nature* **227,** 680–685
28. Adams, P. D., Grosse-Kunstleve, R. W., Hung, L. W., Ioerger, T. R., McCoy, A. J., Moriarty, N. W., Read, R. J., Sacchettini, J. C., Sauter, N. K., and Terwilliger, T. C. (2002) *Acta Crystallogr. D. Biol. Crystallogr.* **58,** 1948–1954
29. Vagin, A., and Teplyakov, A. (2000) *Acta Crystallogr. D. Biol. Crystallogr.* **56,** 1622–1624
30. Perrakis, A., Morris, R., and Lamzin, V. S. (1999) *Nat. Struct. Biol.* **6,** 458–463
31. Emsley, P., and Cowtan, K. (2004) *Acta Crystallogr. D. Biol. Crystallogr.* **60,** 2126–2132
32. Murshudov, G. N., Vagin, A. A., and Dodson, E. J. (1997) *Acta Crystallogr. D. Biol. Crystallogr.* **53,** 240–255
33. Brunger, A. T., Adams, P. D., Clore, G. M., Delano, W. L., Gros, P., Grosse-Kunstleve, R. W., Jiang, J. S., Kuszewski, J., Nilges, M., Pannu, N. S., Read, R. J., Rice, L. M., Simonson, T., and Warren, G. L. (1998) *Acta Crystallogr. D. Biol. Crystallogr.* **54,** 905–921
34. McCoy, A. J., Grosse-Kunstleve, R. W., Storoni, L. C., and Read, R. J. (2005) *Acta Crystallogr. D. Biol. Crystallogr.* **61,** 458–464
35. Inocencio, N. M., Moehring, J. M., and Moehring, T. J. (1994) *J. Biol. Chem.* **269,** 31831–31835
36. Hessler, J. L., and Kreitman, R. J. (1997) *Biochemistry* **36,** 14577–14582
37. Masignani, V., Balducci, E., Serruto, D., Veggi, D., Arico, B., Comanducci, M., Pizza, M., and Rappuoli, R. (2004) *Int. J. Med. Microbiol.* **293,** 471–478
38. Perentesis, J. P., Miller, S. P., and Bodley, J. W. (1992) *Biofactors* **3,** 173–184
39. Armstrong, S., and Merrill, A. R. (2001) *Anal. Biochem.* **292,** 26–33
40. Leppla, S. H., Martin, O. C., and Muehl, L. A. (1978) *Biochem. Biophys. Res. Commun.* **81,** 532–538
41. Chung, D. W., and Collier, R. J. (1977) *Infect. Immun.* **16,** 832–841
42. Beattie, B. K., and Merrill, A. R. (1996) *Biochemistry* **35,** 9042–9051
43. Middlebrook, J. L., and Dorland, R. B. (1977) *Can. J. Microbiol.* **23,** 183–189
44. May, P., Woldt, E., Matz, R. L., and Boucher, P. (2007) *Ann. Med.* **39,** 219–228
45. Kounnas, M. Z., Morris, R. E., Thompson, M. R., FitzGerald, D. J., Strickland, D. K., and Saelinger, C. B. (1992) *J. Biol. Chem.* **267,** 12420–12423
46. Collier, R. J. (2001) *Toxicon* **39,** 1793–1803
47. Tamplin, M. L., Gauzens, A. L., Huq, A., Sack, D. A., and Colwell, R. R. (1990) *Appl. Environ. Microbiol.* **56,** 1977–1980
48. Kirn, T. J., Jude, B. A., and Taylor, R. K. (2005) *Nature* **438,** 863–866
49. Chiron, M. F., Fryling, C. M., and FitzGerald, D. J. (1994) *J. Biol. Chem.* **269,** 18167–18176
50. Yates, S. P., Taylor, P. L., Jorgensen, R., Ferraris, D., Zhang, J., Andersen, G. R., and Merrill, A. R. (2005) *Biochem. J.* **385,** 667–675
51. Jorgensen, R., Merrill, A. R., Yates, S. P., Marquez, V. E., Schwan, A. L., Boesen, T., and Andersen, G. R. (2005) *Nature* **436,** 979–984
52. Ogata, M., Chaudhary, V. K., Pastan, I., and FitzGerald, D. J. (1990) *J. Biol. Chem.* **265,** 20678–20685
53. Lory, S., and Collier, R. J. (1980) *Infect. Immun.* **28,** 494–501
54. Galloway, D. R., Hedstrom, R. C., Mcgowan, J. L., Kessler, S. P., and Wozniak, D. J. (1989) *J. Biol. Chem.* **264,** 14869–14873
55. Kondo, T., FitzGerald, D., Chaudhary, V. K., Adhya, S., and Pastan, I. (1988) *J. Biol. Chem.* **263,** 9470–9475
56. Lyczak, J. B., Cannon, C. L., and Pier, G. B. (2000) *Microbes Infect.* **2,** 1051–1060
57. Tang, H. B., DiMango, E., Bryan, R., Gambello, M., Iglewski, B. H., Goldberg, J. B., and Prince, A. (1996) *Infect. Immun.* **64,** 37–43
58. Makri, S., Purdy, A. E., Bartlett, D. H., and Fierer, J. (2007) *Microbes Infect.* **9,** 1351–1358
59. Hilbi, H., Weber, S. S., Ragaz, C., Nyfeler, Y., and Urwyler, S. (2007) *Environ. Microbiol.* **9,** 563–575
60. Li, M., Dyda, F., Benhar, I., Pastan, I., and Davies, D. R. (1995) *Proc. Natl. Acad. Sci. U. S. A* **92,** 9308–9312
61. Li, M., Dyda, F., Benhar, I., Pastan, I., and Davies, D. R. (1996) *Proc. Natl. Acad. Sci. U. S. A* **93,** 6902–6906